J of Nuclear Medicine Technology, first published online February 7, 2023 as doi:10.2967/jnmt.122.264990

Optimization of the attenuation coefficient for Chang's attenuation correction in ^{123}I brain perfusion single-photon emission computed tomography

Taisuke Murata[1, 2], Yuri Hayashi[1], Masahisa Onoguchi[2], Takayuki Shibutani[2], Takashi Iimori[1], Koichi Sawada[1], Tetsuro Umezawa[1], Yoshitada Masuda[1], Takashi Uno[3]

1. Department of Radiology, Chiba University Hospital, Chiba 260-8677, Japan
2. Department of Quantum Medical Technology, Graduate School of Medical Sciences, Kanazawa University, 5-11-80 Kodatsuno, Kanazawa, Ishikawa 920-0942, Japan
3. Department of Diagnostic Radiology and Radiation Oncology, Graduate School of Medicine, Chiba University, Chiba 260-8670, Japan

Corresponding author: Masahisa Onoguchi
Department of Quantum Medical Technology, Graduate School of Medical Sciences, Kanazawa University, 5-11-80 Kodatsuno, Kanazawa, Ishikawa 920-0942, Japan
Phone: +81-76-265-2526, Fax: +81-76-265-2526
E-mail: onoguchi@staff.kanazawa-u.ac.jp

Short running title: Attenuation coefficient in brain SPECT

Word count: 6000

Abstract

N-isopropyl-p-[^{123}I]-iodoamphetamine (^{123}I-IMP) brain perfusion single-photon emission computed tomography (SPECT) has been employed with various attenuation coefficients (μ-values); however, optimization is required. This study aimed to determine the optimal μ-value for Chang's attenuation correction (AC) (Chang's method) using clinical data by comparing Chang's method and the computed tomography (CT)-based AC (CT-based method).

Methods: We used 100 patients (normal group: 60, disease group: 40) who underwent ^{123}I-IMP SPECT. SPECT images of the normal group were obtained to calculate the AC using Chang's method (μ-values: 0.07–0.20, 0.005 interval) and the CT-based method, both without scatter correction (SC) (ChangAC, CTAC) and with SC (ChangACSC, CTACSC), respectively. The optimal μ-value (μ_{opt}-value) with the smallest mean %error for the brain regions of normal group was calculated. Agreement between Chang's and the CT-based methods applying the μ_{opt}-value was evaluated using Bland–Altman analysis. Additionally, the %error in the region of hypoperfusion in the diseased group was compared to the %error in the same region in the normal group when the μ_{opt}-value was applied.

Results: The μ_{opt}-values were 0.140 for ChangAC and 0.160 for ChangACSC. In Chang's

method, with the μ_{opt}-value applied, fixed and proportional biases were observed in the Bland–Altman analysis (both $P<0.05$), and there was a tendency for the %error to be underestimated in the limbic regions and overestimated in the central brain regions. No significant difference between the disease group and the normal group in the region of hypoperfusion in either ChangAC or ChangACSC.

Conclusions: The present study revealed that the μ_{opt}-values of Chang's method are ChangAC: 0.140 and ChangACSC: 0.160.

Keywords: single-photon emission computed tomography, brain perfusion, Chang's attenuation correction

Introduction

Brain perfusion single-photon emission computed tomography (SPECT) is required to be qualitatively and quantitatively accurate. SPECT projection data are subject to scattering and attenuation of gamma rays caused by the subject. Particularly, attenuation causes a depth-dependent decrease in counts within the subject, leading to significant accuracy errors in quantitative evaluation (*1*). Therefore, attenuation correction (AC) is vital to obtain accurate brain perfusion SPECT images.

Computed tomography (CT)-based AC (CT-based method), a non-uniform AC, and Chang's attenuation correction (Chang's method), a uniform AC, are mainly used in brain perfusion SPECT. The CT-based method is considered the gold standard for AC because of its high correction accuracy. Contrastingly, Chang's method is widely used in routine clinical practice primarily because of its simplicity in AC processing. It does not require a CT scan, thereby eliminating radiation exposure. The attenuation map of Chang's method is given by a constant attenuation coefficient (μ-value) for each radionuclide energy. Various μ-values have been employed for ^{123}I-IMP brain perfusion SPECT, with variations: broad-beam: 0.07 (*2*), 0.08 (*3*), 0.09 (*4*), 0.10 (*5*); narrow-beam: 0.11 (*3*), 0.12 (*6*), 0.146 (*2*,*5*,*7*), 0.160 (*8*), 0.166 (*9*), 0.167 (*10*). Optimization of μ-values for Chang's method in ^{123}I-IMP brain

perfusion SPECT is required.

It is necessary to consider the effect of skull attenuation (*11*–*13*) and the difference in μ-value depending on the slice position (*9*,*12*,*14*) to optimize the μ-value of Chang's method. The skull is relatively thicker in the occipital region than in other regions (*15*), making it difficult to reproduce the actual skull thickness in the phantom accurately. Additionally, when μ-values are determined using a pooled phantom, the basal ganglia level is the evaluation target (*16*), resulting in inadequate evaluation of the parietal and cerebellar levels. Van Laere et al. (*13*,*17*) noted that μ-values determined experimentally using phantoms cannot be directly extrapolated for application to clinical data.

This study aimed to determine the optimal μ-value (μ_{opt}-value) using clinical data. The μ-value that most closely approximates the AC effect of the CT-based method, the gold standard, was determined as the μ_{opt}-value of Chang's method. We further validated the μ_{opt}-value by evaluating the agreement between Chang's and the CT-based methods when the μ_{opt}-values were applied and the error of the μ_{opt}-values in hypoperfusion regions.

Materials and Methods

This retrospective study was approved by our institution's ethics review committee. All

the data used for analysis were obtained from routine clinical diagnoses investigations; no other examinations were performed for the study. The requirement for written consent was waived by the ethics review committee.

Patients

This study included 100 patients (male: 47, female: 53; median age: 66.0 [23.1–90.3] years) who underwent ^{123}I-IMP brain perfusion SPECT examination between January and December 2021. Patients diagnosed with generally preserved perfusion or mild nonspecific hypoperfusion were defined as the normal group. Patients diagnosed with specific hypoperfusion were defined as the disease group. The normal group included 60 patients (male: 28, female: 32; median age: 63.5 [23.1–90.3] years), and the disease group included 40 patients (male: 19, female: 21; median age: 72.5 [48.4–88.2] years). Disease groups included Alzheimer's disease (AD), dementia with Lewy bodies (DLB), frontotemporal lobar degeneration (FTLD), and multiple system atrophy of the cerebellar type (MSA-C), with 10 patients each. Patients with diseases other than the above and equivocal hypoperfusion were excluded from selecting the disease groups.

Data acquisition and reconstruction

All patients were administered 111 MBq of ^{123}I-IMP, and the SPECT scan was performed using a dual-head gamma camera (NM/CT 870 DR hybrid SPECT/CT scanner; GE Healthcare, Chicago, IL) equipped with an extended low-energy general-purpose collimator. The energy peak was set at 159 keV with a 20% energy window. The sub-window for scatter correction (SC) was set at 20% centered at 130 keV. SPECT scans were obtained with the following parameters: continuous-acquisition mode, 360° circular orbit, 90 projections of a 4° step angle, 180 s acquisition per cycle for eight cycles, radius rotation of 150 mm, 64 × 64 matrices with a zoom magnification of 2.0×. CT scans for AC were obtained with the following acquisition/reconstruction parameters: helical scan mode, tube voltage of 120 kVp, tube current of 40 mA, 0.5 s of the rotation time, and slice thickness of 3.75 mm (matrix, 512×512; pixel size, 0.97 mm). The CT data were converted with bilinear scaling to attenuation maps corresponding to 159 keV using the scanner software.

All patient SPECT projection data were reconstructed using ordered subset expectation maximization (OSEM; five iterations and ten subsets). For each patient, OSEM + Chang's method (ChangAC), OSEM + Chang's method + SC (ChangACSC), OSEM + CT-based method (CTAC), and OSEM + CT-based method + SC (CTACSC) was reconstructed.

For ChangAC and ChangACSC, AC was performed by varying the μ-values from 0.07 to 0.20 (0.05 intervals). A threshold process for each patient determined the contour of the attenuation map when performing Chang's method. The threshold value whose contour was nearest to the outer edge of the skull was adopted by referring to the CT images (*12*). The dual-energy window (DEW) method was used for SC (*18*). The pixel size of the reconstructed SPECT image was 4.42 mm, and the slice thickness was also 4.42 mm. A Butterworth filter (cutoff, 0.5 cycles/cm; order, 8) was used for smoothing.

Data analysis

All SPECT images were analyzed using AZE Virtual Place HAYABUSA software (Canon Medical Systems, Otawara-shi, Tochigi, Japan), and three-dimensional stereotactic surface projection (3D-SSP) analysis was performed. To avoid anatomical standardization errors, the head tilt was adjusted to the anterior commissure - posterior commissure line (AC-PC line) (*19,20*). Counts of 37 brain regions were measured using volume-of-interest (VOI) templates incorporated into the 3D-SSP on anatomically standardized SPECT images. The 37 brain regions included were the left and right parietal lobes, temporal lobe, frontal lobe, occipital lobe, posterior cingulate gyrus, anterior cingulate gyrus, medial frontal lobe, medial

parietal lobe, medial temporal lobe, sensorimotor cortex, visual cortex, caudate nucleus, cerebellum, cerebellar vermis, putamen, parahippocampal gyrus, amygdala, thalamus, and pons (not divided into left and right).

Determination of optimal attenuation coefficients

The %error of each brain region for ChangAC/CTAC pairs and ChangACSC/CTACSC pairs was calculated for the normal group. The %error was calculated using the following equation:

$$\%\ \text{Error} = \frac{\text{Count}_{\text{ChangAC,ChangACSC}} - \text{Count}_{\text{CTAC,CTACSC}}}{\text{Count}_{\text{CTAC,CTACSC}}}$$

First, the mean %error for all brain regions (37 VOIs) was calculated for each patient. The μ-value with the smallest mean %error was the optimal μ-value for each patient. The number distribution of the optimal μ-values for each patient was determined to identify the range of individual differences.

Next, the mean %error of all brain regions (2,220 VOIs) in the 60 normal patients was calculated. The μ-value with the smallest mean %error was defined as the μ_{opt}-value. The absolute value of the %error in each brain region was also calculated to identify the magnitude of the error. Additionally, unsuitable μ-values with significant differences from those of the CT-based method were identified by comparing the counts of all brain regions

in ChangAC/CTAC pairs and ChangACSC/CTACSC pairs.

Bland–Altman analysis was performed on each pair of counts to evaluate the agreement between ChangAC (with μ_{opt}-value)/CTAC pairs and between ChangACSC (with μ_{opt}-value)/CTACSC pairs. The %error of each pair was also identified for each brain region.

Validation of optimal attenuation coefficients

SPECT images of the disease group with ChangAC and ChangACSC with μ_{opt}-values were used. The %error in the hypoperfusion region for the ChangAC/CTAC and ChangACSC/CTACSC pairs was calculated and compared to the %error in the same region in the normal group. The hypoperfusion regions were defined as AD: posterior cingulate gyrus and medial temporal lobe; DLB: occipital lobe; FTLD: frontal and temporal lobes; MSA-C: cerebellum.

Statistical analysis

Statistical analyses were performed using JMP Pro (version 16.1.0; SAS Institute, Cary, NC). The difference in counts between ChangAC and CTAC pairs, ChangACSC and CTACSC pairs with varying μ-values for Chang's method was evaluated using the Wilcoxon

signed-rank test. Fixed and proportional biases for ChangAC/CTAC pairs and ChangACSC/CTACSC pairs were evaluated using Bland–Altman analysis. A paired *t*-test and linear regression analysis were used to analyze the fixed and proportional biases on the Bland–Altman plots, respectively. The %error of the disease and normal groups for ChangAC/CTAC pairs and ChangACSC/CTACSC pairs in the hypoperfusion region was evaluated using the Wilcoxon signed-rank test. For all statistical analyses, $p<0.05$ was considered statistically significant.

Results

The distribution of the number of optimal μ-values per patient in the normal group is shown in Fig. 1. The optimal μ-value differed for each patient. In ChangAC, the optimal μ-value was distributed in the range of 0.125–0.150, with 0.140 as the most common optimal μ-value. In ChangACSC, the optimal μ-value was distributed in the range 0.145–0.180, with 0.160 and 0.165 as the most common optimal μ-values.

The %error of ChangAC in the normal group is listed in Table 1, and Table 2 shows the %error of ChangACSC. ChangAC exhibited the smallest %error with CTAC with a μ-value of 0.140, whereas ChangACSC displayed the smallest %error with CTACSC with a μ-

value of 0.160. For both ChangAC and ChangACSC, smaller μ-values tended to underestimate counts, and larger μ-values resulted in overestimated counts. The maximum absolute %error was 22.81% for ChangAC with the μ-value of 0.140 and 31.63% for ChangACSC with the μ-value of 0.160. Comparison of counts between Chang and the CT-based method revealed significant differences in all μ-values except 0.140 for ChangAC and 0.160 and 0.165 for ChangACSC.

The results of the agreement between ChangAC applying μ_{opt}-value: 0.140 and CTAC, ChangACSC applying μ_{opt}-value: 0.160 and CTACSC in the normal group are shown in Fig. 2a, b. We identified a positive fixed bias between ChangAC and CTAC and a negative fixed bias between ChangACSC and CTACSC (both $P<0.05$). Therefore, there was an overall overestimation trend for ChangAC and an underestimation trend for ChangACSC. Linear regression analysis revealed a proportional bias for ChangAC and ChangACSC (both $P<0.05$).

The %error in each brain region for ChangAC applying μ_{opt}-value: 0.140 and CTAC, and ChangACSC applying μ_{opt}-value: 0.160 and CTACSC in the normal group is shown in Fig. 3. In both ChangAC and ChangACSC, some brain regions in the limbic region (bilateral parietal lobes, right temporal lobe, right frontal lobe, bilateral occipital lobes, right

sensorimotor cortex, bilateral visual cortex) were underestimated, and some brain regions in the central region (bilateral medial temporal lobes, bilateral caudate nucleus, pons, bilateral putamen, bilateral parahippocampal gyrus, bilateral thalamus) tended to be overestimated.

Examples of SPECT images of normal patients with ChangAC and CTAC, ChangACSC and CTACSC are shown in Fig. 4a, b. ChangAC and ChangACSC tended to slightly overestimate the central brain regions and underestimate the limbic cortex in the μ_{opt}-value in series normalization. In CT-based method normalization, the μ_{opt}-value produced SPECT images more similar to the CT-based method than the conventionally used μ-values.

Table 3 summarizes the results of the evaluation of the %error in the hypoperfusion region for the ChangAC applying μ_{opt}-value: 0.140 and ChangACSC applying μ_{opt}-value: 0.160. The %error in the hypoperfusion region for each disease group was not significantly different from that of the same region in the normal group for either ChangAC or ChangACSC.

Discussion

We determined μ_{opt}-values in ChangAC and ChangACSC retrospectively using clinical data. The μ_{opt}-values were ChangAC: 0.140 and ChangACSC: 0.160. However, some

brain regions were under- or over-estimated in the SPECT images when the μ_{opt}-values were applied. Limitations of Chang's method, as a uniform AC, were also revealed.

The distribution of optimal μ-values per patient displayed some variation, centered around ChangAC: 0.140, ChangACSC: 0.160 and 0.165. However, it is not practical to apply individual μ-values for each patient. Therefore, we determined μ_{opt}-values by averaging out the variation in patients by analyzing all brain regions together in 60 normal patients. By comparing the counts of Chang's method with those of the CT-based method, we identified significant differences for all μ-values except 0.140 in ChangAC and 0.160 and 0.165 in ChangACSC, thereby providing statistical support for the μ_{opt}-value. Stodilka et al. (*12*) reported a relative quantification error of 20% by applying a μ-value of 0.120 to ChangAC in a phantom study. In the present patient-based study, the absolute %error for ChangAC applying the μ_{opt}-value was 22.81%. Although the degree of error was comparable, the optimal μ-values for phantoms and patients were observed to be different. As reports of quantitation using ^{123}I, Iida et al. reported a maximum %error of 30% for ChangAC with μ-value of 0.090 and ChangACSC with μ value of 0.166 (9). For ChangAC, a smaller %error was achieved by applying the μ_{opt}-value in this study. For ChangACSC, there was no noticeable difference from this study because the μ-values were close to our μ_{opt}-values.

Interindividual variability of anatomical standardization in brain perfusion SPECT is 3–9% (*21-23*). The absolute %error between the CT-based and Chang's methods in the present study averaged 4.45% for ChangAC and 6.37% for ChangACSC. Applying the μ_{opt}-values achieved AC error comparable to the interindividual variation of anatomical standardization that can occur in routine clinical practice.

Bland–Altman analysis revealed systematic bias in ChangAC and ChangACSC when applying the μ_{opt}-value, and agreement with the CT-based method was not perfect. The %error for ChangAC and ChangACSC tended to be underestimated in the limbic brain regions and overestimated in the central brain regions. This trend was visually confirmed in an example of the SPECT image of a normal patient shown in Fig. 4. Ito et al. (*4*) reported an overestimation of central brain regions in ChangACSC applying a μ-value of 0.166, relatively close to our μ_{opt}-value. These facts highlight the limitations of Chang's method even when using μ_{opt}-values and reiterate the superiority of the CT-based method.

The skull possesses a higher μ-value than brain tissue due to greater photon loss. Further, the thickness of the skull varies slightly with age and sex (*24*). The different optimal μ-values per patient in the present study appear to be due to skull thickness variations among patients. Nicholson et al. (*11*) reported that the skull paradoxically affects broad-beam μ-

values, and other studies (*12*,*13*) also reported lower μ-values than those of uniform soft tissue. Stodilka et al. (*12*) observed that optimal μ-values at the cerebellar level, surrounded by thick bony structures, are smaller than those at the basal ganglia level. Iida et al. (*9*) reported smaller μ-values at the cerebellar level, where the airway is included in the slice position, and higher μ-values at the parietal level, where the skull is relatively thick. These reports indicate a complex interplay of several factors involved in optimizing μ-values. In this study, we averaged the optimal μ-values differing per patient by a combined analysis of 60 patients and accounted for differences in correction error among brain regions by analyzing all brain regions together using anatomical standardization. Our method provides a generalizable μ_{opt}-value that considers differences in skull thickness (an error factor for inter-patient variation) and differences in attenuation structure for each imaging slice position (an error factor for intra-patient variation). Consequently, the μ_{opt}-value determined in the present study is relatively high compared to the various μ-values conventionally used.

The theoretical narrow-beam μ-value for water for the 159 keV γ rays emitted by ^{123}I is 0.148 (*25*). Using the theoretical narrow-beam μ-value for ChangAC overcorrects for attenuation and overestimates the brain center region (*26*). Harris et al. (*27*) reported that a slightly lower μ-value should be applied than the theoretical μ-value. Here, the μ_{opt}-value of

ChangAC was also lower than the theoretical narrow-beam μ-value.

The μ_{opt}-value of ChangACSC in our study was higher than the theoretical narrow-beam μ-value, whereas previous studies proposed lower values than the theoretical narrow-beam μ-value (*12*,*13*,*16*). Some previous studies using phantoms focused on assessing uniformity of AC (*12*,*16*) because brain perfusion SPECT images are commonly normalized by the maximum count in the series. The uniformity of AC contributes to qualitative improvement. In this study using clinical data, the standard deviation (SD) of the %error at low μ-values was small, and uniformity within the series was preserved. Contrarily, the absolute %error applying μ_{opt}-values was comparable to that reported by Stodilka et al. (*12*), indicating that quantification was assured. Iida et al. (*9*) reported no apparent difference in regional CBF images obtained with the measured attenuation map and the ChangACSC applying a high μ-value of 0.166. Therefore, it is difficult for Chang's method to achieve both qualitative and quantitative performance because low μ-values contribute to qualitative improvement, whereas high μ-values contribute to quantitative improvement. Since the degree of contribution of high μ-values to the quantitation improvement was greater than the degree of contribution of low μ-values to the qualitative improvement, using high μ-values is recommended.

We validated the μ_{opt}-value determined using the normal group in hypoperfusion regions to confirm their adaptability to the disease group. The choice of target diseases was considered so that the entire brain region (anterior, posterior, lateral, parietal, and basal regions) could be included as hypoperfusion regions. We observed no significant difference in the %error in the hypoperfusion regions in the normal and disease groups when the μ_{opt}-value was applied, indicating adaptability of the μ_{opt}-value for the disease group.

The normal group used in the present study included patients who underwent routine clinical examinations and not normal volunteers. However, conducting studies on normal volunteers is not practical to determine optimal μ-values. Licho et al. (*28*) also evaluated patients who underwent routine clinical examinations to validate the effects of various AC methods. In clinical routine, there are few patients in whom brain perfusion is generally preserved. We included patients diagnosed with a mild degree of nonspecific hypoperfusion in the normal group to obtain a larger cohort of patients for inclusion in the present study. Additionally, including more patients enables more generalizable μ_{opt}-values to be determined.

This study had some limitations. First, it was difficult for all patients to achieve an ideal head tilt because of patient-specific limitations in body position during SPECT imaging.

These factors may have influenced the variation of μ_{opt}-values depending on the slice position. Second, the specifications for SC of the SPECT/CT system used in this study were limited to the DEW method only. Since ^{123}I also emits photons with energies as high as 529 keV, it is best to use a multiple-window method, including the triple energy window method, to improve the effects of down scatter. Third, we investigated using one type of gamma camera for ^{123}I with constant parameters for image reconstruction and SC. A preliminary validation using several patients confirmed that the optimal μ-values for each patient did not change when the number of iterations for image reconstruction and the weighting factor for SC was changed; however, this was not sufficient. The possibility that μ_{opt}-values may change when other radionuclides, gamma cameras, or other SC are used cannot be extrapolated to other clinical applications. These should be investigated in further studies.

5. Conclusions

We evaluated the optimal μ-value for Chang's method using clinical data by comparing it with the CT-based method. It was determined that the μ_{opt}-values of Chang's method were 0.140 for ChangAC and 0.160 for ChangACSC. It was possible to achieve mean AC accuracies of 4.45% for ChangAC and 6.37% for ChangACSC using μ_{opt}-values.

Disclosure

No potential conflict of interest relevant to this article was reported.

Acknowledgments

We would like to thank Editage (www.editage.com) for English language editing.

Key points

QUESTION: Can we optimize the μ-value of Chang's method using clinical data?

PERTINENT FINDINGS: In this retrospective study, we determined the optimal μ-value for Chang's method by comparing this method with the computed tomography-based method, the gold standard for attenuation correction (AC). We found that the optimal μ-values were 0.140 for Chang's method without scatter correction (SC) and 0.160 for Chang's method with SC, although various μ-values have been used in previous studies.

IMPLICATIONS FOR PATIENT CARE: Chang's method can achieve more accurate AC using our determined μ-values.

References

1. Zaidi H, Hasegawa B. Determination of the attenuation map in emission tomography. *J Nucl Med*. 2003;44:291–315.
2. Hayashi M, Deguchi J, Utsunomiya K, et al. Comparison of methods of attenuation and scatter correction in brain perfusion SPECT. *J Nucl Med Technol.* 2005;33:224–229.
3. Inoue Y, Hara T, Ikari T, Takahashi K, Miyatake H, Abe Y. Super-early images of brain perfusion SPECT using (123)I-IMP for the assessment of hyperperfusion in stroke patients. *Ann Nucl Med.* 2018;32:695–701.
4. Ito H, Iida H, Kinoshita T, Hatazawa J, Okudera T, Uemura K. Effects of scatter correction on regional distribution of cerebral blood flow using I-123-IMP and SPECT. *Ann Nucl Med.* 1999;13:331–336.
5. Shiga T, Kubo N, Takano A, et al. The effect of scatter correction on 123I-IMP brain perfusion SPET with the triple energy window method in normal subjects using SPM analysis. *Eur J Nucl Med Mol Imaging.* 2002;29:342–345.
6. Yamashita K, Uchiyama Y, Ofuji A, et al. Fully automatic input function determination program for simple noninvasive (123)I-IMP microsphere cerebral blood flow quantification method. *Phys Med.* 2016;32:1180–1185.

7. Ishii K, Hanaoka K, Okada M, et al. Impact of CT attenuation correction by SPECT/CT in brain perfusion images. *Ann Nucl Med.* 2012;26:241–247.
8. Iida H, Nakagawara J, Hayashida K, et al. Multicenter evaluation of a standardized protocol for rest and acetazolamide cerebral blood flow assessment using a quantitative SPECT reconstruction program and split-dose 123I-iodoamphetamine. *J Nucl Med.* 2010;51:1624–1631.
9. Iida H, Narita Y, Kado H, et al. Effects of scatter and attenuation correction on quantitative assessment of regional cerebral blood flow with SPECT. *J Nucl Med.* 1998;39:181–189.
10. Kim KM, Watabe H, Hayashi T, et al. Quantitative mapping of basal and vasareactive cerebral blood flow using split-dose 123I-iodoamphetamine and single photon emission computed tomography. *Neuroimage.* 2006;33:1126–1135.
11. Nicholson R, Doherty M, Wilkins K, Prato F. Paradoxical effects of the skull on attenuation correction requirements for brain SPECT. *J Nucl Med.* 1988; 29:1316.
12. Stodilka RZ, Kemp BJ, Prato FS, Nicholson RL. Importance of bone attenuation in brain SPECT quantification. *J Nucl Med.* 1998;39:190–197.
13. Van Laere K, Koole M, Versijpt J, Dierckx R. Non-uniform versus uniform attenuation

correction in brain perfusion SPET of healthy volunteers. *Eur J Nucl Med*. 2001;28:90–98.

14. Arlig A, Gustafsson A, Jacobsson L, Ljungberg M, Wikkelsö C. Attenuation correction in quantitative SPECT of cerebral blood flow: a Monte Carlo study. *Phys Med Biol.* 2000;45:3847–3859.
15. Law SK. Thickness and resistivity variations over the upper surface of the human skull. *Brain Topogr.* 1993;6:99–109.
16. Kemp BJ, Prato FS, Dean GW, Nicholson RL, Reese L. Correction for attenuation in technetium-99m-HMPAO SPECT brain imaging. *J Nucl Med.* 1992;33:1875–1880.
17. Van Laere K, Koole M, Kauppinen T, Monsieurs M, Bouwens L, Dierck R. Nonuniform transmission in brain SPECT using 201Tl, 153Gd, and 99mTc static line sources: anthropomorphic dosimetry studies and influence on brain quantification. *J Nucl Med.* 2000;41:2051–2062.
18. Jaszczak RJ, Greer KL, Floyd CE, Jr., Harris CC, Coleman RE. Improved SPECT quantification using compensation for scattered photons. *J Nucl Med.* 1984;25:893–900.
19. Onishi H, Matsutake Y, Kawashima H, Matsutomo N, Amijima H. Comparative study of anatomical normalization errors in SPM and 3D-SSP using digital brain phantom. *Ann*

Nucl Med. 2011;25:59–67.

20. Minoshima S, Koeppe RA, Mintun MA, et al. Automated detection of the intercommissural line for stereotactic localization of functional brain images. *J Nucl Med.* 1993;34:322–329.
21. Imran MB, Kawashima R, Sato K, et al. Mean regional cerebral blood flow images of normal subjects using technetium-99m-HMPAO by automated image registration. *J Nucl Med.* 1998;39:203-207.
22. Jonsson C, Pagani M, Johansson L, Thurfjell L, Jacobsson H, Larsson SA. Reproducibility and repeatability of 99Tcm-HMPAO rCBF SPET in normal subjects at rest using brain atlas matching. *Nucl Med Commun*. 2000;21:9–18.
23. Catafau AM, Lomeña FJ, Pavia J, et al. Regional cerebral blood flow pattern in normal young and aged volunteers: a 99mTc-HMPAO SPET study. *Eur J Nucl Med.* 1996;23:1329–1337.
24. Lillie EM, Urban JE, Lynch SK, Weaver AA, Stitzel JD. Evaluation of skull cortical thickness changes with age and sex from computed tomography scans. *J Bone Miner Res.* 2016;31:299–307.
25. Berger MJ, Hubbell JH. "XCOM: Photon cross sections on a personal computer." NBSIR

87–3597 (National Bureau of Standards (US), 1987).

26. Zaidi H, Montandon ML. Which attenuation coefficient to use in combined attenuation and scatter corrections for quantitative brain SPET? *Eur J Nucl Med Mol Imaging*. 2002;29:967–969; author reply 9–70.

27. Harris CC, Greer KL, Jaszczak RJ, Floyd CE, Jr., Fearnow EC, Coleman RE. Tc-99m attenuation coefficients in water-filled phantoms determined with gamma cameras. *Med Phys*. 1984;11:681–685.

28. Licho R, Glick SJ, Xia W, Pan TS, Penney BC, King MA. Attenuation compensation in 99mTc SPECT brain imaging: a comparison of the use of attenuation maps derived from transmission versus emission data in normal scans. *J Nucl Med.* 1999;40:456–463.

Figure Legends

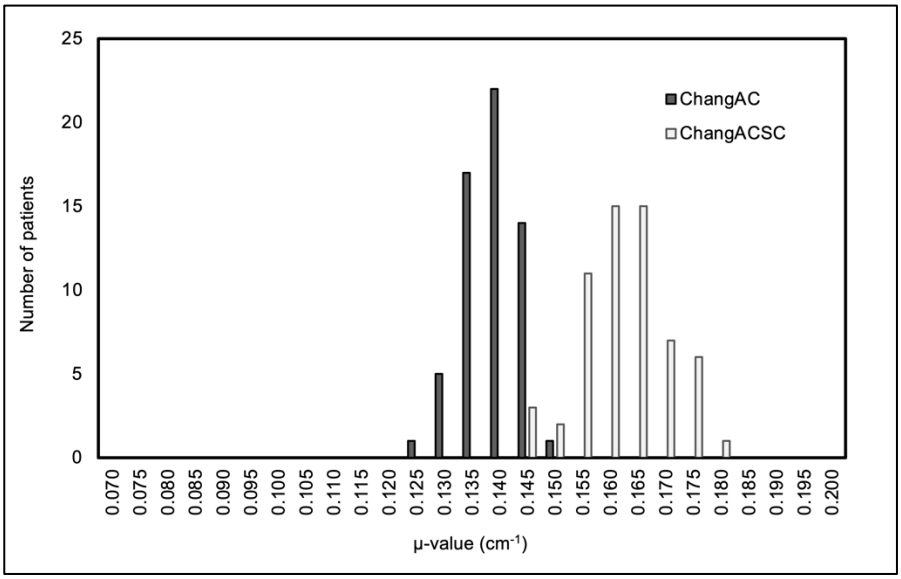

Fig. 1 Distribution of the number of optimal μ-values per patient in the normal group

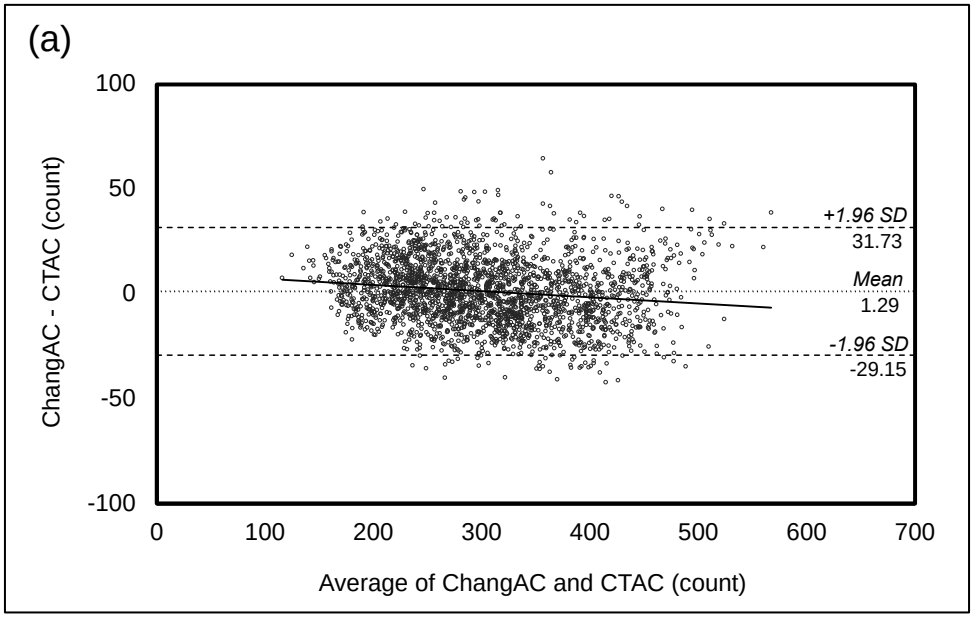

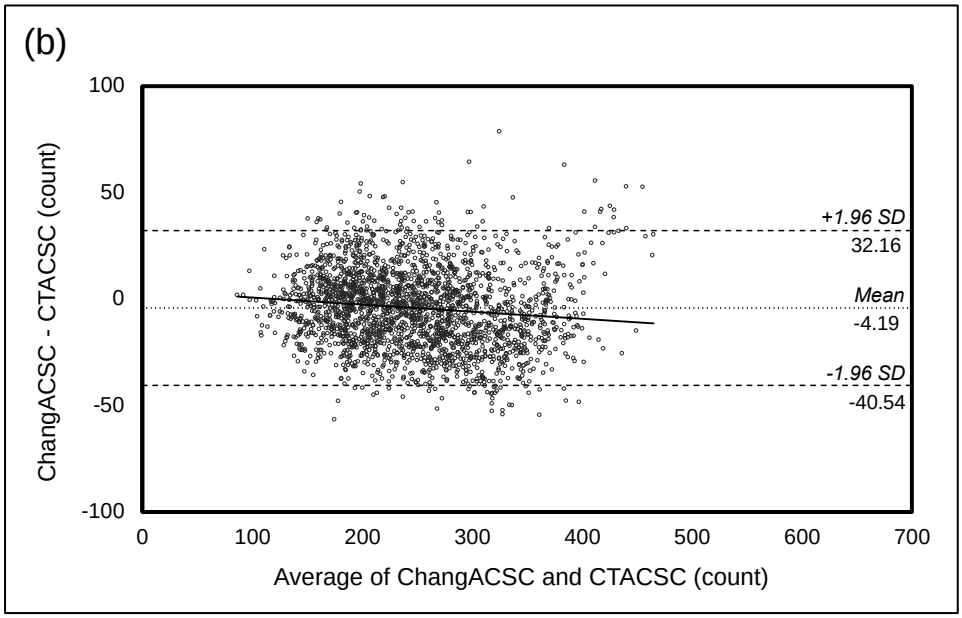

Fig. 2 Results of Bland–Altman analysis comparing (a) ChangAC applying μ_{opt}-value: 0.140 and CTAC, and (b) ChangACSC applying μ_{opt}-value: 0.160 and CTACSC in the normal

group. The vertical axis shows the difference in counts, and the horizontal axis shows the mean value of counts. The dotted line represents the mean value, (a): 1.29, (b): -4.19. Solid lines show regressions. The 95% limits of agreement are represented by dashed lines, (a): -29.15 - 31.73, (b): -40.54 - 32.16. The 95% confidence intervals were (a): 0.66, 1.92 and (b): -4.95, -3.44. Abbreviations: ChangAC, Chang's attenuation correction without scatter correction; CTAC, computed tomography-based attenuation correction without scatter correction; ChangACSC, Chang's attenuation correction with scatter correction; CTACSC, computed tomography-based attenuation correction with scatter correction

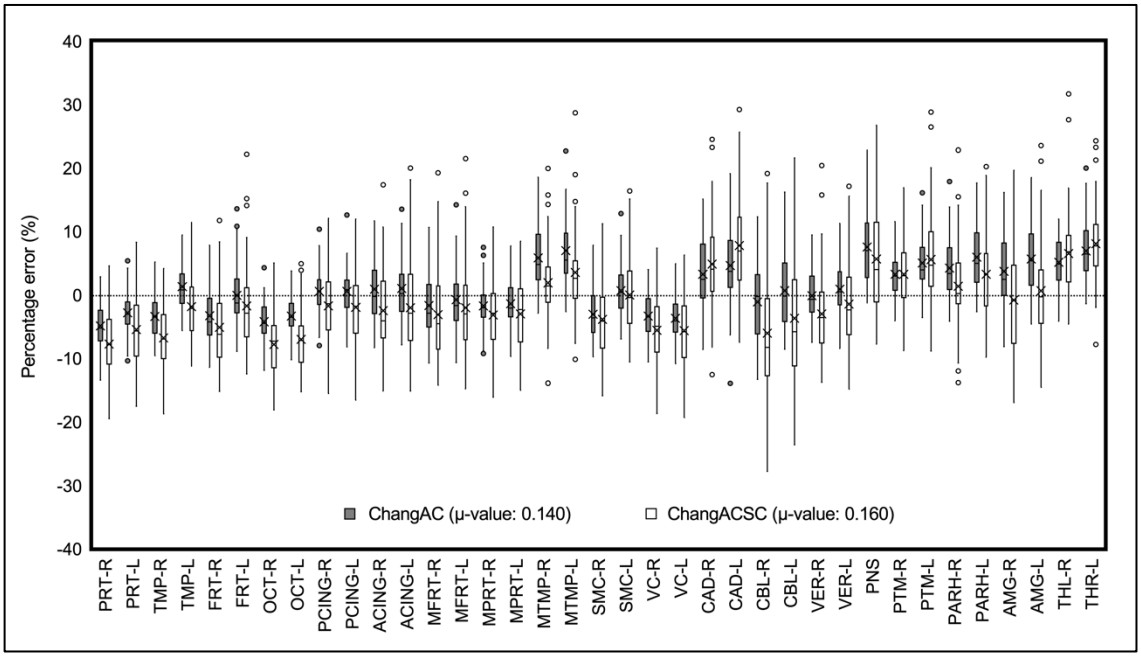

Fig. 3 The %error in each brain region for ChangAC applying μ_{opt}-value: 0.140 and CTAC, for ChangACSC applying μ_{opt}-value: 0.160 and CTACSC in the normal group. Dotted lines indicate zero. For ChangAC and ChangACSC, limbic brain regions tended to be underestimated, and central brain regions overestimated

Abbreviations: PRT-R, right parietal lobe; PRT-L, left parietal lobe; TMP-R, right temporal lobe; TMP-L, left temporal lobe; FRT-R, right frontal lobe; FRT-L, left frontal lobe; OCT-R, right occipital lobe; OCT-L, left occipital lobe; PCING-R, right posterior cingulate gyrus; PCING-L, left posterior cingulate gyrus; ACING-R, right anterior cingulate gyrus; ACING-L, left anterior cingulate gyrus; MFRT-R, right medial frontal lobe; MFRT-L, left medial

frontal lobe; MPRT-R, right medial parietal lobe; MPRT-L, left medial parietal lobe; MTMP-R, right medial temporal lobe; MTMP-L, left medial temporal lobe; SMC-R, right sensorimotor cortex; SMC-L, left sensorimotor cortex; VC-R, right visual cortex; VC-L, left visual cortex; CAD-R, right caudate nucleus; CAD-L, left caudate nucleus; CBL-R, right cerebellum; CBL-L, left cerebellum; VER-R, right cerebellar vermis; VER-L, left cerebellar vermis; PNS, pons; PTM-R, right putamen; PTM-L, left putamen; PARH-R, right parahippocampal gyrus; PARH-L, left parahippocampal gyrus; AMG-R, right amygdala; AMG-L, left amygdala; THL-R, right thalamus; THR-L, left thalamus

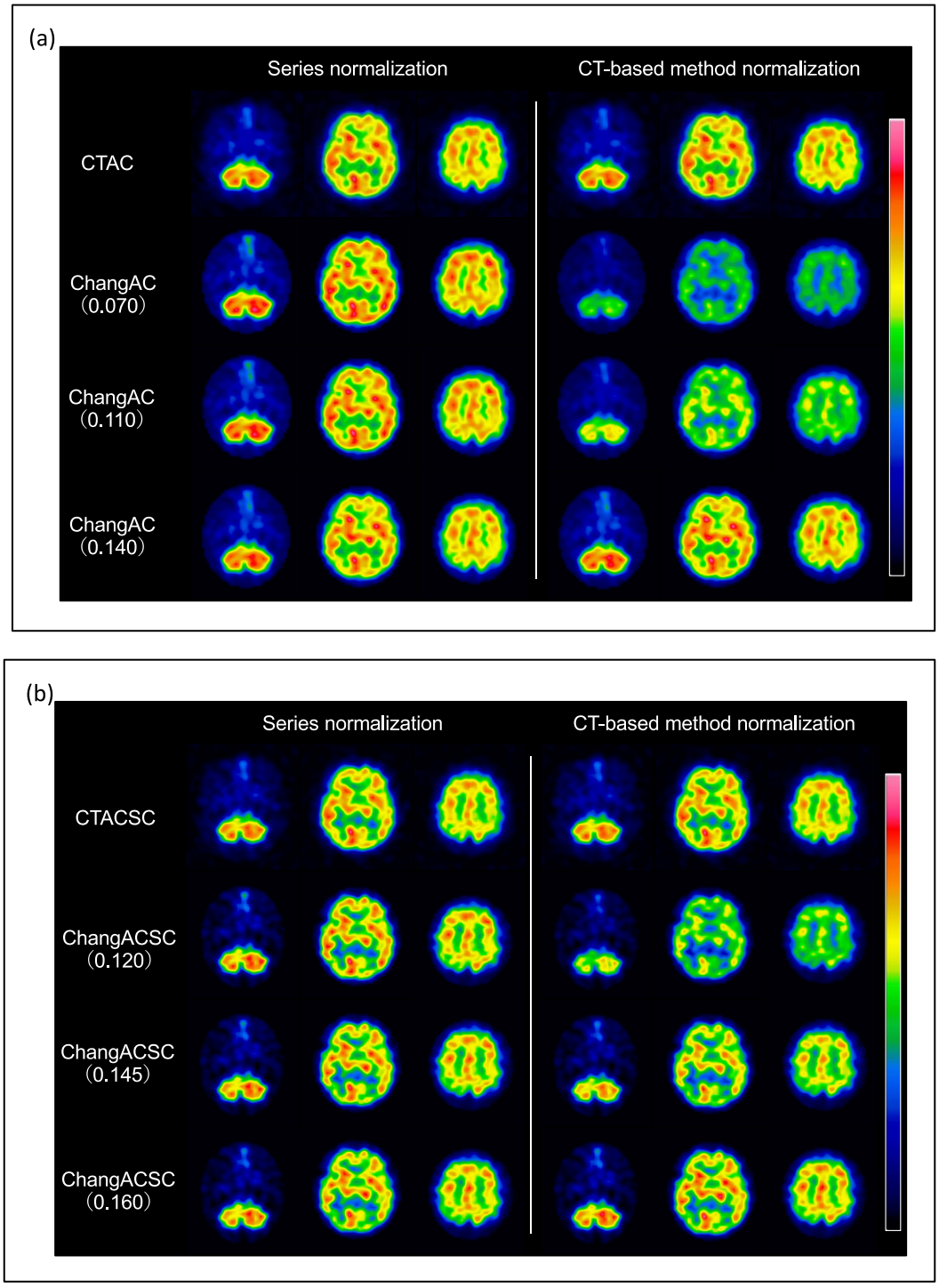

Fig. 4 Comparison of SPECT images of (a) CTAC and ChangAC and (b) CTACSC and ChangACSC in one normal patient. For ChangAC, μ-values: 0.07, 0.110, and 0.140; for

ChangACSC, μ-values: 0.12, 0.145, and 0.160 were applied. The left side of the solid line shows SPECT images normalized by the maximum counts in a series (series normalization), and the right side shows SPECT images normalized by the maximum counts of the CT-based method (CT-based method normalization). The axial slices are shown from left to right at the cerebellar level, basal ganglia level, and parietal level, respectively. Abbreviation: CT, computed tomography; CTAC, computed tomography-based attenuation correction without scatter correction; ChangAC, Chang's attenuation correction without scatter correction; CTACSC, computed tomography-based attenuation correction with scatter correction; ChangACSC, Chang's attenuation correction with scatter correction

Table 1. The %error and absolute %error between ChangAC applying each μ-value and CTAC

μ-value	%error	Absolute %error	P-value
0.070	-38.22 ± 4.02 (-46.17, -29.28)	38.22 ± 4.02 (29.28, 46.17)	<0.05
0.075	-36.13 ± 3.90 (-46.51, -28.14)	36.13 ± 3.90 (28.14, 46.51)	<0.05
0.080	-33.78 ± 3.85 (-42.76, -25.84)	33.78 ± 3.85 (25.84, 42.76)	<0.05
0.085	-31.40 ± 3.64 (-41.03, -22.94)	31.40 ± 3.64 (22.94, 41.03)	<0.05
0.090	-28.75 ± 3.66 (-39.59, -19.08)	28.75 ± 3.66 (19.08, 39.59)	<0.05
0.095	-26.24 ± 3.34 (-36.81, -19.01)	26.24 ± 3.34 (19.01, 36.81)	<0.05
0.100	-23.78 ± 3.10 (-35.49, -16.19)	23.78 ± 3.10 (16.19, 35.49)	<0.05
0.105	-21.01 ± 3.03 (-32.43, -12.95)	21.01 ± 3.03 (12.95, 32.43)	<0.05
0.110	-18.24 ± 2.79 (-32.14, -9.23)	18.24 ± 2.79 (9.23, 32.14)	<0.05
0.115	-15.40 ± 2.50 (-25.94, -6.05)	15.40 ± 2.50 (6.05, 25.94)	<0.05
0.120	-12.12 ± 3.59 (-25.31, 1.84)	12.12 ± 3.59 (0.16, 25.31)	<0.05
0.125	-9.00 ± 3.94 (-22.25, 7.01)	9.07 ± 3.78 (0.06, 22.25)	<0.05
0.130	-5.85 ± 4.40 (-19.93, 14.24)	6.38 ± 3.58 (0.00, 19.93)	<0.05
0.135	-2.45 ± 4.95 (-17.42, 18.89)	4.54 ± 3.13 (0.00, 18.89)	<0.05
0.140	**0.96 ± 5.62 (-13.92, 22.81)**	**4.45 ± 3.57 (0.00, 22.81)**	0.58
0.145	4.18 ± 6.78 (-10.06, 28.65)	6.14 ± 5.07 (0.00, 28.65)	<0.05
0.150	8.13 ± 6.93 (-8.82, 35.49)	8.58 ± 6.37 (0.00, 35.49)	<0.05

0.155	11.95 ± 7.74 (-6.43, 38.81)	12.06 ± 7.57 (0.00, 38.81)	<0.05
0.160	15.86 ± 8.57 (-3.87, 49.12)	15.87 ± 8.54 (0.13, 49.12)	<0.05
0.165	19.92 ± 8.88 (-1.74, 52.43)	19.92 ± 8.87 (0.01, 52.43)	<0.05
0.170	23.93 ± 9.61 (1.83, 56.66)	23.93 ± 9.61 (1.83, 56.66)	<0.05
0.175	28.23 ± 10.50 (4.85, 64.57)	28.23 ± 10.50 (4.85, 64.57)	<0.05
0.180	32.72 ± 11.41 (8.26, 70.96)	32.72 ± 11.41 (8.26, 70.96)	<0.05
0.185	37.16 ± 12.69 (6.29, 82.40)	37.16 ± 12.69 (6.29, 82.40)	<0.05
0.190	42.19 ± 13.82 (13.63, 91.62)	42.19 ± 13.82 (13.63, 91.62)	<0.05
0.195	46.63 ± 14.82 (13.69, 99.40)	46.63 ± 14.82 (13.69, 99.40)	<0.05
0.200	52.23 ± 16.26 (20.34, 107.87)	52.23 ± 16.26 (20.34, 107.87)	<0.05

1 The error is represented by mean ± standard deviation (minimum, maximum). The smallest
2 mean %error and absolute %error are shown in bold. ChangAC, Chang's attenuation
3 correction without scatter correction; CTAC, computed tomography-based attenuation
4 correction without scatter correction
5

Table 2. The %error and absolute %error between ChangACSC applying each μ-value and CTACSC

μ-value	%error	Absolute %error	P-value
0.070	-45.25 ± 5.28 (-60.55, -23.14)	45.25 ± 5.28 (23.14, 60.55)	<0.05
0.075	-43.35 ± 5.31 (-61.10, -21.36)	43.35 ± 5.31 (21.36, 61.10)	<0.05
0.080	-41.39 ± 5.34 (-56.87, -18.13)	41.39 ± 5.34 (18.13, 56.87)	<0.05
0.085	-39.25 ± 5.31 (-53.72, -15.78)	39.25 ± 5.31 (15.78, 53.72)	<0.05
0.090	-37.34 ± 5.35 (-55.51, -14.08)	37.34 ± 5.35 (14.08, 55.51)	<0.05
0.095	-35.15 ± 5.34 (-49.77, -11.23)	35.15 ± 5.34 (11.23, 49.77)	<0.05
0.100	-32.88 ± 5.33 (-50.07, -9.59)	32.88 ± 5.33 (9.59, 50.07)	<0.05
0.105	-32.92 ± 7.79 (-56.93, -6.89)	32.92 ± 7.79 (6.89, 56.93)	<0.05
0.110	-28.30 ± 5.44 (-48.50, -5.35)	28.30 ± 5.44 (5.35, 48.50)	<0.05
0.115	-26.04 ± 5.60 (-45.59, -2.26)	26.04 ± 5.60 (2.26, 45.59)	<0.05
0.120	-23.26 ± 5.71 (-43.11, -0.11)	23.26 ± 5.71 (0.11, 43.11)	<0.05
0.125	-20.84 ± 6.01 (-41.59, 3.75)	20.86 ± 5.96 (0.02, 41.59)	<0.05
0.130	-18.40 ± 5.69 (-39.99, 4.84)	18.42 ± 5.61 (0.03, 39.99)	<0.05
0.135	-15.66 ± 5.92 (-36.30, 8.17)	15.74 ± 5.70 (0.02, 36.30)	<0.05
0.140	-13.43 ± 5.85 (-35.95, 10.34)	13.56 ± 5.54 (0.01, 35.95)	<0.05
0.145	-10.56 ± 6.29 (-29.52, 13.57)	10.99 ± 5.51 (0.05, 29.52)	<0.05
0.150	-7.58 ± 6.67 (-29.75, 19.25)	8.65 ± 5.21 (0.01, 29.75)	<0.05

0.155	-4.40 ± 7.33 (-26.91, 26.51)	7.04 ± 4.85 (0.01, 26.91)	<0.05
0.160	**-1.11 ± 7.94 (-27.83, 31.63)**	**6.37 ± 4.88 (0.01, 31.63)**	0.06
0.165	2.26 ± 8.76 (-20.46, 39.34)	6.97 ± 5.76 (0.01, 39.34)	0.05
0.170	5.63 ± 9.40 (-19.51, 42.13)	8.37 ± 7.07 (0.02, 42.13)	<0.05
0.175	9.39 ± 10.45 (-16.02, 50.41)	10.88 ± 8.88 (0.04, 50.41)	<0.05
0.180	12.99 ± 11.28 (-19.97, 62.12)	13.76 ± 10.32 (0.00, 62.12)	<0.05
0.185	17.09 ± 11.83 (-11.97, 64.69)	17.33 ± 11.46 (0.02, 64.69)	<0.05
0.190	20.98 ± 12.77 (-10.09, 69.26)	21.10 ± 12.57 (0.00, 69.26)	<0.05
0.195	24.45 ± 13.11 (-16.22, 72.17)	24.51 ± 12.98 (0.08, 72.17)	<0.05
0.200	28.34 ± 14.13 (-11.36, 86.37)	28.37 ± 14.07 (0.05, 86.37)	<0.05

The error is represented by mean ± standard deviation (minimum, maximum). The smallest mean %error and absolute %error are shown in bold. CTACSC, computed tomography-based attenuation correction with scatter correction; ChangACSC, Chang's attenuation correction with scatter correction

Table 3. Comparison of the %error between the hypoperfusion region in each disease group and the same region in the normal group for ChangAC applying μ_{opt}-value: 0.140 and ChangACSC applying μ_{opt}-value: 0.160

Disease	Brain region		ChangAC			ChangACSC		
			Disease	Normal	P-value	Disease	Normal	P-value
AD	Posterior cingulate gyrus	Rt	0.55 ± 3.49	-0.71 ± 3.04	0.34	-3.71 ± 2.78	-1.76 ± 5.72	0.14
		Lt	0.52 ± 3.44	0.17 ± 2.48	0.83	-4.85 ± 4.19	-1.97 ± 5.75	0.13
	Medial temporal lobe	Rt	3.00 ± 3.32	5.82 ± 4.76	0.08	-0.55 ± 4.36	1.89 ± 6.26	0.23
		Lt	4.83 ± 3.38	6.95 ± 5.03	0.18	2.38 ± 3.64	3.51 ± 6.57	0.83
DLB	Occipital lobe	Rt	-4.24 ± 3.38	-4.33 ± 2.57	0.89	-7.82 ± 5.09	-7.47 ± 4.97	0.69
		Lt	-3.33 ± 2.96	-2.89 ± 3.10	0.64	-7.03 ± 4.64	-6.33 ± 3.66	0.44
FTLD	Frontal lobe	Rt	-3.29 ± 4.34	-3.79 ± 1.41	0.85	-5.15 ± 6.02	-5.26 ± 0.86	0.80
		Lt	-0.09 ± 4.45	-1.39 ± 2.05	0.56	-1.76 ± 6.75	-2.89 ± 4.25	0.84
	Temporal lobe	Rt	-2.70 ± 3.48	-3.43 ± 3.16	0.59	-5.98 ± 4.51	-1.45 ± 4.66	0.88
		Lt	1.64 ± 3.30	1.27 ± 3.26	0.70	-1.45 ± 4.66	-1.88 ± 4.89	0.88
MSA-C	Cerebellum	Rt	-1.11 ± 5.51	-0.13 ± 3.40	0.69	-6.05 ± 9.54	-8.79 ± 4.63	0.45
		Lt	0.66 ± 5.83	2.32 ± 3.71	0.36	-3.70 ± 9.93	-6.62 ± 4.76	0.72

The error is represented by mean ± standard deviation.

ChangAC, Chang's attenuation correction without scatter correction; ChangACSC, Chang's attenuation correction with scatter correction; Rt, right; Lt, left; AD, Alzheimer's disease; DLB, dementia with Lewy bodies; FTLD, frontotemporal lobar degeneration; MSA-C, multiple system atrophy of the cerebellar type

1 Graphical Abstract

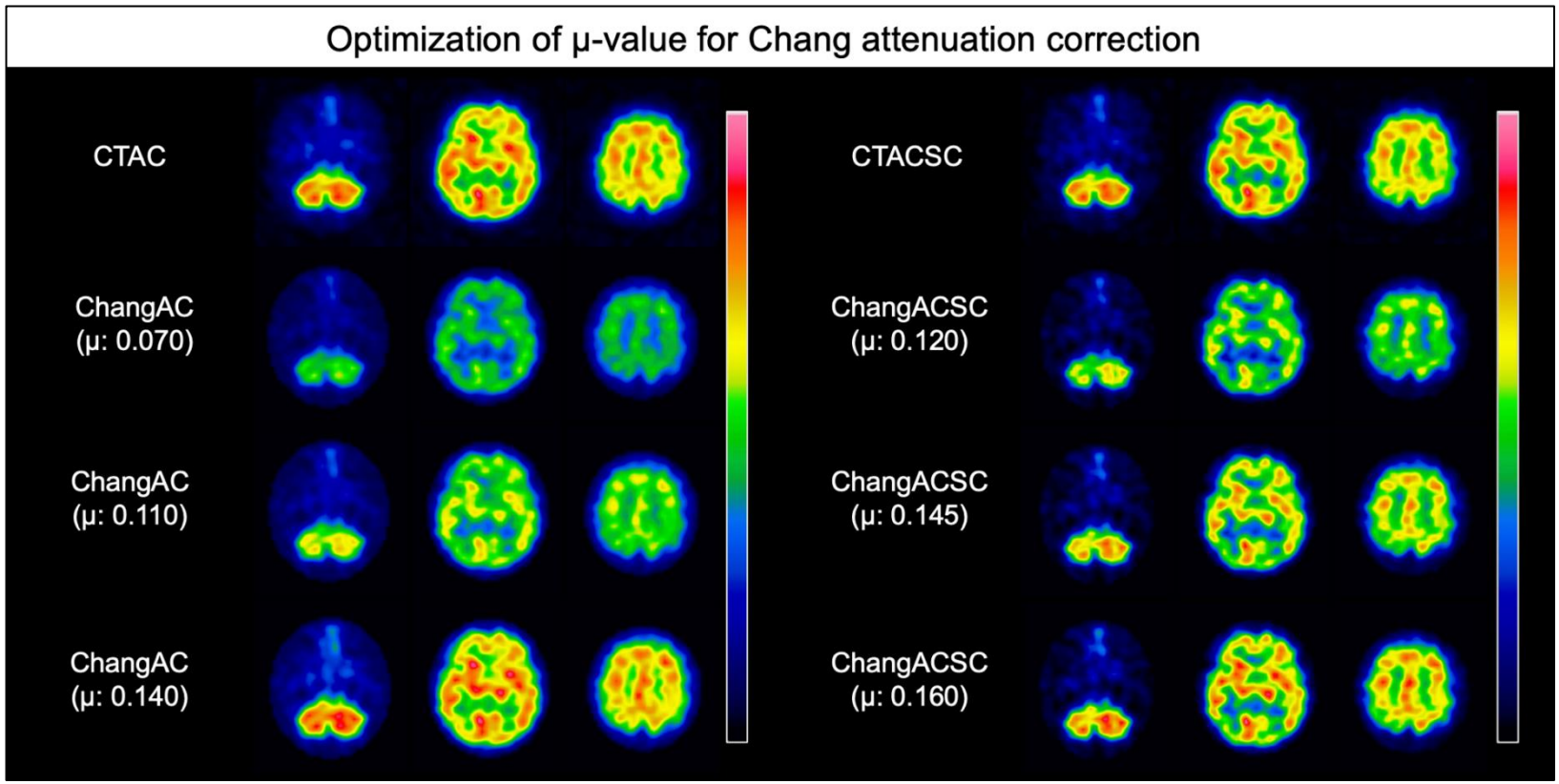

2